Proceedings of The 2024 IEEE International
Conference on Real-time Computing and Robotics
June 24 - 28, 2024

2024 IEEE International Conference on Real-time Computing and Robotics (RCAR) | 979-8-3503-7260-1/24/$31.00 ©2024 IEEE | DOI: 10.1109/RCAR61438.2024.10671184

Nonlinear Output Feedback Control for Double-Pendulum Aerial Transportation Systems with Variable-Length Cable

Hai Yu, Yang Wang, Bingbing Liu, Jianda Han, Yongchun Fang and Xiao Liang

***Abstract*— Implementing aerial transportation systems in real-world scenarios is becoming feasible. Due to the ability to dynamically adjust the distance between quadrotor and cargo, the aerial transportation system with variable-length cable (ATSVC) holds significant value in applications such as tunnel traversal and obstacle avoidance. However, existing studies often overlook the hook, which means that the double-pendulum effect is ignored. In practical systems, there exists complex dynamic coupling among the motion of quadrotor, variations in cable length, and the swing motion of hook and cargo. Besides, the velocity information in real-world environments cannot be accurately measured, which makes precise control extremely challenging. To address the aforementioned challenges, this paper introduces an output feedback control method for the double-pendulum ATSVC. Specifically, the proposed method operates without the need for velocity information and effectively constrains the quadrotor's overshoot within a prescribed scope. Lyapunov techniques and LaSalle's Invariance Theorem are employed to prove the stability of the closed-loop system. Numerical simulations are implemented to verify the proposed method's performance.**

I. INTRODUCTION

With the continuous maturation of unmanned aerial vehicle (UAV) technology, leveraging UAVs for aerial cargo transportation has become feasible. In particular, due to their low design costs, cable-suspended transportation methods have become widely employed for aerial transportation of crops, rescue equipment, construction materials, etc.

Recently, researchers have conducted extensive studies on the cable-suspended aerial transportation systems (ATSs). Yang *et al.* [1] develop a cascade control framework by using nonsingularity terminal sliding-based control technique and super-twisting-based control for quadrotor's attitude and position, respectively. Akhtar *et al.* [2] utilize a nonlinear coordinate transformation to convert the dynamic model of the ATS into an exact linear form, based on which a path tracking controller is designed to ensure the cargo converges to a specified path and achieves path invariance. By mounting a camera on the quadrotor, Guo *et al.* [3] design an image-based visual servoing approach to achieve picking up, transfer, and release of unknown mass cargo. Employing the finite-time disturbance observer, Yu *et al.* [4] design a fault-tolerant control that enables precise positioning of the quadrotor and suppression of cargo swing angles even in the event of blade damage.

However, the previously mentioned ATSs all utilize fixed-length cables, posing challenges for application in certain specialized scenarios such as tunnel crossings and obstacle avoidance. To enhance the flexibility and applicability, some recent studies have also developed ATS with variable-length cable (ATSVC) [5]–[7]. Based on the established coordinate-free dynamic model, Zeng *et al.* [5] propose a nonlinear geometric control law, which can track quadrotor attitude, cargo attitude and position, and cable length. By designing a cable length adjustment mechanism, Liang *et al.* [6] achieve the first physical experimental verification of the system with variable-length cable. Furthermore, by using a coupling signal that combines quadrotor position and cargo swing angles, Huang *et al.* [7] aim to improve the cargo swing elimination ability. It is worth noting that the aforementioned ATSVC all overlook the hook. In practical systems, a hook is typically attached to the end of the cable to facilitate the replacement of suspended cargo. However, the presence of a hook in the system introduces the double-pendulum effect, significantly increasing the challenge of precise control. Currently, research on the double-pendulum effect primarily focuses on systems with fixed-length cable [8]–[10]. To this end, this paper studies the double-pendulum ATSVC. Compared to ATSs with fixed-length cable neglecting the hook, the inclusion of variable-length cable and hook swing increases the system's degrees of freedom, resulting in significantly stronger nonlinearity and more complex dynamic coupling.

To tackle the aforementioned challenges, this paper initially establishes the dynamic model of the double-pendulum ATSVC. Subsequently, an output feedback control scheme is devised based on energy analysis. Notably, considering that velocity signal measurements in practical systems often suffer from cumulative errors, the controller proposed in this paper operates independently of velocity signals. Moreover, to prevent collisions between the system and its surrounding environment during flight, an overshoot constraint term is integrated into the controller to confine the overshoot within a prescribed scope. The convergence of the equilibrium point is demonstrated using Lyapunov techniques and LaSalle's Invariance Theorem. Finally, the effectiveness of the proposed method is validated through numerical simulations.

The rest of this paper is organized as follows. In Section II, we present the problem formulation. Section III provides

*This work was supported in part by National Natural Science Foundation of China under Grant 623B2054, Grant 62273187, Grant 62233011 and Grant U20A20198, in part by the Fundamental Research Funds for the Central Universities under Grant 63241576 and in part by the Natural Science Foundation of Tianjin under Grant 23JCQNJC01930. *(Corresponding author: Xiao Liang)*

The authors are with the Institute of Robotics and Automatic Information System, College of Artificial Intelligence, and also with the Tianjin Key Laboratory of Intelligent Robotics, Nankai University, Tianjin 300350, China {yuhai, wangy1893, liubingbing}@mail.nankai.edu.cn; {hanjianda, fangyc, liangx}@nankai.edu.cn

the main results. Subsequently, simulation results are given to show the performance of the proposed control scheme in Section IV. Finally, Section V summarizes the paper.

II. PROBLEM FORMULATION

A. Dynamic Model

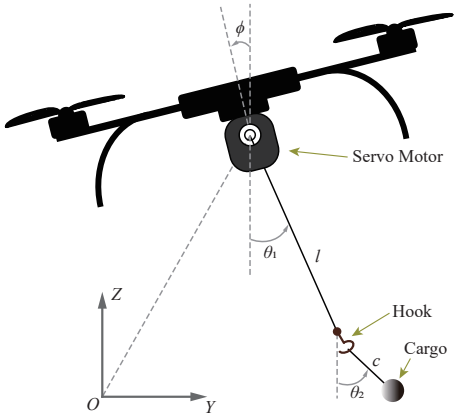

Fig. 1: The schematic diagram of double-pendulum ATSVC.

The illustration of the double-pendulum ATSVC is shown in Fig. 1. A servo motor is mounted at the center of mass of the quadrotor which is utilized to adjust the cable length. A hook is attached to the end of the cable, and the cargo is suspended from the hook. $M, m_h, m_c \in \mathbb{R}$ denote the quadrotor, hook and cargo masses. $g \in \mathbb{R}$ is the gravitational acceleration. $l(t) \in \mathbb{R}$ denotes the cable length. The distance between the hook and the cargo is denoted by $c \in \mathbb{R}$. $\boldsymbol{\xi}(t) = [y(t), z(t)]^\top \in \mathbb{R}^2$ denotes the quadrotor position. $\theta_1(t), \theta_2(t) \in \mathbb{R}$ are swing angles of the hook and cargo. $\phi(t) \in \mathbb{R}$ is the quadrotor's roll angle. $f \in \mathbb{R}$ is the thrust input of the quadrotor. $f_l \in \mathbb{R}$ is the input of the servo motor. To facilitate the subsequent model description and analysis, let C_1, S_1, C_2, S_2, C_{1-2}, S_{1-2}, C_ϕ, S_ϕ denote the abbreviations of $\cos\theta_1$, $\sin\theta_1$, $\cos\theta_2$, $\sin\theta_2$, $\cos(\theta_1-\theta_2)$, $\sin(\theta_1-\theta_2)$, $\cos\phi$, $\sin\phi$. According to some recent research of various transportation systems [1], [4], [7], [11], the following assumption is given as:

Assumption 1: The swing angles of the hook and cargo satisfy $-\frac{\pi}{2} < \theta_1, \theta_2 < \frac{\pi}{2}$.

Based on the Lagrangian modeling method, the dynamic model of double-pendulum ATSVC can be formulated as follows:

$$\begin{aligned}
&(M+m_h+m_c)\,\ddot{y} + (m_h+m_c)\left(\ddot{l}S_1 + 2\dot{l}\dot{\theta}_1 C_1\right)\\
&+ (m_h+m_c)\,l\left(\ddot{\theta}_1 C_1 - \dot{\theta}_1^2 S_1\right) + m_c c\left(\ddot{\theta}_2 C_2 - \dot{\theta}_2^2 S_2\right)\\
&= -fS_\phi, \qquad (1)\\
&(M+m_h+m_c)\,\ddot{z} - (m_h+m_c)\left(\ddot{l}C_1 - 2\dot{l}\dot{\theta}_1 S_1\right)\\
&+ (m_h+m_c)\,l\left(\ddot{\theta}_1 S_1 + \dot{\theta}_1^2 C_1\right) + m_c c\left(\ddot{\theta}_2 S_2 + \dot{\theta}_2^2 C_2\right)\\
&+ (M+m_h+m_c)\,g = fC_\phi, \qquad (2)\\
&(m_h+m_c)\left(\ddot{y}S_1 - \ddot{z}C_1 + \ddot{l} - l\dot{\theta}_1^2 - gC_1\right) + m_c c\left(S_{1-2}\ddot{\theta}_2\right.\\
&\left.-\dot{\theta}_2^2 C_{1-2}\right) = f_l, \qquad (3)\\
&(m_h+m_c)\,l\left(\ddot{y}C_1 + \ddot{z}S_1 + l\ddot{\theta}_1 + 2\dot{l}\dot{\theta}_1 + gS_1\right)\\
&+ m_c l c\left(\dot{\theta}_2^2 S_{1-2} + \ddot{\theta}_2 C_{1-2}\right) = 0, \qquad (4)\\
&m_c c\left(\ddot{y}C_2 + \ddot{z}S_2 + l\ddot{\theta}_1 C_{1-2} + c\ddot{\theta}_2 + \ddot{l}S_{1-2} + 2\dot{l}\dot{\theta}_1 C_{1-2}\right.\\
&\left.-l\dot{\theta}_1^2 S_{1-2} + gS_2\right) = 0. \qquad (5)
\end{aligned}$$

Define the generalized vector $\boldsymbol{q} = [y, z, l, \theta_1, \theta_2]^\top \in \mathbb{R}^5$, and then the above dynamic equations can be summarized in the following manner:

$$M_c(\boldsymbol{q})\ddot{\boldsymbol{q}} + V_c(\boldsymbol{q}, \dot{\boldsymbol{q}})\dot{\boldsymbol{q}} + \boldsymbol{G}(\boldsymbol{q}) = \boldsymbol{F}, \qquad (6)$$

where $M_c(\boldsymbol{q}) \in \mathbb{R}^{5\times5}$, $V_c(\boldsymbol{q}, \dot{\boldsymbol{q}}) \in \mathbb{R}^{5\times5}$, $\boldsymbol{G}(\boldsymbol{q}) \in \mathbb{R}^5$, $\boldsymbol{F} = \left[\boldsymbol{u}^\top, 0, 0\right]^\top = [-fS_\phi, fC_\phi, f_l, 0, 0]^\top \in \mathbb{R}^5$ are inertia matrix, Centripetal-Coriolis matrix, gravity vector, and force vector. $\boldsymbol{u} \in \mathbb{R}^3$ is the to-be-designed control input. M_c and V_c satisfy the skew-symmetric relationship, i.e., $\boldsymbol{x}^\top\left(\frac{1}{2}\dot{M}_c - V_c\right)\boldsymbol{x} = 0,\ \forall\ \boldsymbol{x} \in \mathbb{R}^5$.

B. Control Objective

The control objective is to design a feedback control scheme that drives the quadrotor to the desired position $\boldsymbol{\xi}_d = [y_d, z_d]^\top$ and adjusts the cable to the desired length l_d, while eliminating the hook and the cargo swing simultaneously, i.e.,

$$y \to y_d, z \to z_d, l \to l_d, \theta_1 \to 0, \theta_2 \to 0. \qquad (7)$$

Based on the above control objective, the error signals are defined as $\boldsymbol{e}_\eta = [e_y, e_z, e_l]^\top = [y, z, l]^\top - [y_d, z_d, l_d]^\top$, $\dot{\boldsymbol{e}}_\eta = [\dot{y}, \dot{z}, \dot{l}]^\top$.

III. MAIN RESULTS

A. Controller Design

The energy function of the system is provided as follows:

$$E = \frac{1}{2}\dot{\boldsymbol{q}}^\top M_c \dot{\boldsymbol{q}} + (m_h+m_c)\,gl\,(1-C_1) + m_c gc\,(1-C_2)\,. \qquad (8)$$

Utilizing the skew-symmetric relationship, and inserting (6) into the time derivative of (8), one has

$$\begin{aligned}\dot{E} =&\dot{\boldsymbol{q}}^{\top}\left(M_c\ddot{\boldsymbol{q}}+\frac{1}{2}\dot{M}_c\dot{\boldsymbol{q}}\right)+(m_h+m_c)\,g\dot{l}\,(1-C_1)\\&+(m_h+m_c)\,gl\dot{\theta}_1S_1+m_cgc\dot{\theta}_2S_2\\=&\dot{\boldsymbol{e}}_{\eta}^{\top}\left[\boldsymbol{u}-(M+m_h+m_c)\,g\boldsymbol{r}_2+(m_h+m_c)\,g\boldsymbol{r}_3\right],\end{aligned}\tag{9}$$

where $\boldsymbol{r}_2=[0,1,0]^{\top}$, $\boldsymbol{r}_3=[0,0,1]^{\top}$. Furthermore, construct the following scaler function:

$$\begin{aligned}E_p =&E+\sum_{i=y,z,l}k_{pi}\left[e_i\arctan(e_i)-\frac{1}{2}\ln(1+e_i^2)\right]\\&+\sum_{i=y,z,l}\frac{k_{si}e_i^2}{2\left[\left(|i_d-i_0|+\delta_i\right)^2-(i-i_0)^2\right]},\end{aligned}\tag{10}$$

where $k_{pi},k_{si}\in\mathbb{R}_+,i=y,z,l$ are positive control gains. $\delta_i,i=y,z,l$ represents the allowable overshoot magnitude. Taking the time derivative of (10) yeilds

$$\begin{aligned}\dot{E}_p =&\dot{\boldsymbol{e}}_{\eta}^{\top}\left[\boldsymbol{u}-(M+m_h+m_c)\,g\boldsymbol{r}_2+(m_h+m_c)\,g\boldsymbol{r}_3\right.\\&\left.+K_p\mathrm{Arctan}(\boldsymbol{e}_{\eta})+K_s\boldsymbol{\chi}\right],\end{aligned}\tag{11}$$

where $K_p=\mathrm{diag}([k_{py},k_{pz},k_{pl}])\in\mathbb{R}_+^{3\times3}$ and $K_s=\mathrm{diag}([k_{sy},k_{sz},k_{sl}])\in\mathbb{R}_+^{3\times3}$ are positive gain matrices, $\mathrm{Arctan}(\boldsymbol{e}_{\eta})=[\arctan(e_y),\arctan(e_z),\arctan(e_l)]^{\top}$, $\boldsymbol{\chi}=[\chi_y,\chi_z,\chi_l]^{\top}$, $\chi_i=\frac{e_i\left[(|i_d-i_0|+\delta_i)^2-(i-i_0)(i_d-i_0)\right]}{\left[(|i_d-i_0|+\delta_i)^2-(i-i_0)^2\right]^2},i=y,z,l.$

Thus, according to (11), an output feedback control scheme can be constructed as:

$$\begin{aligned}\boldsymbol{u} =&-K_p\mathrm{Arctan}(\boldsymbol{e}_{\eta})-K_d\mathrm{Arctan}(\boldsymbol{\epsilon}_{\eta})-K_s\boldsymbol{\chi}\\&+(M+m_h+m_c)\,g\boldsymbol{r}_2-(m_h+m_c)\,g\boldsymbol{r}_3,\end{aligned}\tag{12}$$

where $K_d=\mathrm{diag}\left([k_{dy},k_{dz},k_{dl}]\right)\in\mathbb{R}_+^{3\times3}$ is the gain matrix, $\boldsymbol{\epsilon}_{\eta}=[\epsilon_y,\epsilon_z,\epsilon_l]^{\top}$ is dynamically generated as :

$$\boldsymbol{\epsilon}_{\eta}=\boldsymbol{\sigma}_{\eta}+K_d\boldsymbol{e}_{\eta},\quad\dot{\boldsymbol{\sigma}}_{\eta}=-K_d\boldsymbol{\epsilon}_{\eta},\tag{13}$$

$$\Rightarrow\dot{\boldsymbol{\epsilon}}_{\eta}=-K_d\boldsymbol{\epsilon}_{\eta}+K_d\dot{\boldsymbol{e}}_{\eta},\tag{14}$$

and $\mathrm{Arctan}(\boldsymbol{\epsilon}_{\eta})=[\arctan(\epsilon_y),\arctan(\epsilon_z),\arctan(\epsilon_l)]^{\top}$.

B. Stability Analysis

Theorem 1: The developed control scheme (12) can enable the quadrotor to reach the target position, adjust the cable to the desired length, and effectively suppress the hook and cargo swing, i.e.,

$$\lim_{t\to\infty}[e_y,e_z,e_l,\theta_1,\theta_2]^{\top}=\boldsymbol{0}_{5\times1}.$$

Furthermore, the overshoot of the quadrotor position and cable length are within the following scope:

$$|i(t)-i_0|<|i_d-i_0|+\delta_i,i=y,z,l.\tag{15}$$

Proof: To proof *Theorem 1*, a scaler function is first given as:

$$V=E_p+\sum_{i=y,z,l}k_{di}\left[\epsilon_i\arctan(\epsilon_i)-\frac{1}{2}\ln(1+\epsilon_i^2)\right].\tag{16}$$

Substituting (12) into the time derivative of (16), and noting (14) yields

$$\begin{aligned}\dot{V} =&\dot{E}_p+\dot{\boldsymbol{\epsilon}}_{\eta}^{\top}K_d\mathrm{Arctan}(\boldsymbol{\epsilon}_{\eta})\\=&-\dot{\boldsymbol{e}}_{\eta}^{\top}K_d\mathrm{Arctan}(\boldsymbol{\epsilon}_{\eta})+\left(-\boldsymbol{\epsilon}_{\eta}^{\top}K_d+\dot{\boldsymbol{e}}_{\eta}^{\top}K_d\right)\mathrm{Arctan}(\boldsymbol{\epsilon}_{\eta})\\=&-\boldsymbol{\epsilon}_{\eta}^{\top}K_d\mathrm{Arctan}(\boldsymbol{\epsilon}_{\eta})\le0,\end{aligned}\tag{17}$$

which indicates that $V(t)$ is nonincreasing, i.e.,

$$V(t)\le V(0)\ll+\infty.\tag{18}$$

Assuming that at least one degree of freedom in y,z,l reaches the boundary range described in (15), it can be inferred from (16) that $V(t)\to\infty$, which contradicts with (18). Thus, the condition in (15) holds, and one has

$$\left(|i_d-i_0|+\delta_i\right)^2-(i-i_0)^2>0,i=y,z,l.\tag{19}$$

Then, from (8), (10), (16) and (19), one can obtain that $V(t)\ge0$. Therefore, $V(t)$ is chosen as the Lyapunov function candidate.

Subsequently, by concluding (8), (10), (16) and (17), the following result can be derived that

$$e_y,e_z,e_l,\dot{y},\dot{z},\dot{l},\dot{\theta}_1,\dot{\theta}_2,\boldsymbol{\epsilon}_{\eta}\in\mathcal{L}_{\infty}\Rightarrow y,z,l\in\mathcal{L}_{\infty},\tag{20}$$

$$\frac{k_{si}e_i^2}{2\left[\left(|i_d-i_0|+\delta_i\right)^2-(i-i_0)^2\right]}\in\mathcal{L}_{\infty},i=y,z,l.\tag{21}$$

Further, to verify the boundedness of the control input $\boldsymbol{u}$, the following analyses are provided as: 1) When $e_i\to0\Rightarrow i\to i_d$, which implies $\frac{1}{(|i_d-i_0|+\delta_i)^2-(i-i_0)^2}\in\mathcal{L}_{\infty}$. Thus, $\chi_i\in\mathcal{L}_{\infty}$; 2) When $e_i\nrightarrow0$, from (20) and (21), one can obtain $\frac{1}{(|i_d-i_0|+\delta_i)^2-(i-i_0)^2}\in\mathcal{L}_{\infty}$. So, one has $\chi_i\in\mathcal{L}_{\infty}$. Based on the above analysis, one can achieve $\boldsymbol{\chi}\in\mathcal{L}_{\infty}$. Then, combining (20), one can further deduce $\boldsymbol{u}\in\mathcal{L}_{\infty}$.

Next, LaSalle's Invariance Theorem [12] is employed to accomplish this proof. Define a set Π as

$$\Pi=\left\{(\boldsymbol{e}_{\eta},\theta_1,\theta_2,\boldsymbol{\epsilon}_{\eta},\dot{\boldsymbol{q}})\,|\dot{V}(t)=0\right\},$$

let Λ be the largest invariant set in Π. Thus, it is obvious that in Λ the following conclusion holds:

$$\boldsymbol{\epsilon}_{\eta}=\boldsymbol{\sigma}_{\eta}+K_d\boldsymbol{e}_{\eta}=\boldsymbol{0}_{3\times1}^{\top},\tag{22}$$

which indicates that

$$\begin{aligned}&\left\{\begin{array}{l}\dot{\boldsymbol{\sigma}}_{\eta}=-K_d\boldsymbol{\epsilon}_{\eta}=\boldsymbol{0}_{3\times1},\\\dot{\boldsymbol{\epsilon}}_{\eta}=-K_d\boldsymbol{\epsilon}_{\eta}+K_d\dot{\boldsymbol{e}}_{\eta}=\boldsymbol{0}_{3\times1},\end{array}\right.\Rightarrow\dot{\boldsymbol{e}}_{\eta}=\boldsymbol{0}_{3\times1},\\\Rightarrow&\dot{y}=0,\dot{z}=0,\dot{l}=0,\ddot{y}=0,\ddot{z}=0,\ddot{l}=0,e_y=\alpha_y,\\&e_z=\alpha_z,e_l=\alpha_l,\end{aligned}\tag{23}$$

where $\alpha_y,\alpha_z,\alpha_l\in\mathbb{R}$ represent the undetermined constants. Substituting the results in (23) and the control law (12) into

(1)–(3), one has

$$(m_h+m_c)\frac{\mathrm{d}}{\mathrm{d}t}\left(l\dot{\theta}_1C_1\right)+m_cc\frac{\mathrm{d}}{\mathrm{d}t}\left(\dot{\theta}_2C_2\right)= -\alpha_y\left(k_{py}+k_{sy}\beta_y\right), \tag{24}$$

$$(m_h+m_c)\frac{\mathrm{d}}{\mathrm{d}t}\left(l\dot{\theta}_1S_1\right)+m_cc\frac{\mathrm{d}}{\mathrm{d}t}\left(\dot{\theta}_2S_2\right)= -\alpha_z\left(k_{pz}+k_{sz}\beta_z\right), \tag{25}$$

$$(m_h+m_c)\left(-l\dot{\theta}_1^2-gC_1\right)+m_cc\left(S_{1-2}\ddot{\theta}_2-\dot{\theta}_2^2C_{1-2}\right)= -\alpha_l\left(k_{pl}+k_{sl}\beta_l\right)-(m_h+m_c)g, \tag{26}$$

where $\beta_i=\frac{\left[(|i_d-i_0|+\delta_i)^2-(i-i_0)(i_d-i_0)\right]}{\left[(|i_d-i_0|+\delta_i)^2-(i-i_0)^2\right]^2}, i=y,z,l$. According to (15) and the fact that $|i_d-i_0|+\delta_i>|i_d-i_0|, i=y,z,l$, one knows

$$\left(|i_d-i_0|+\delta_i\right)^2-(i-i_0)(i_d-i_0)>0. \tag{27}$$

Thus, one can obtain that $\beta_y>0,\beta_z>0,\beta_l>0$, so $k_{py}+k_{sy}\beta_y>0, k_{pz}+k_{sz}\beta_z>0$. Integrating (24) and (25) with respect to time yields

$$(m_h+m_c)\,l\dot{\theta}_1C_1+m_cc\dot{\theta}_2C_2=-\alpha_y\left(k_{py}+k_{sy}\beta_y\right)t+\gamma_y, \tag{28}$$

$$(m_h+m_c)\,l\dot{\theta}_1S_1+m_cc\dot{\theta}_2S_2=-\alpha_z\left(k_{pz}+k_{sz}\beta_z\right)t+\gamma_z, \tag{29}$$

where γ_y,γ_z represent undetermined constants. Moreover, assume that $\alpha_y\neq 0$, if $t\to\infty$, the left hand of (28) tends to ∞, which conflicts with $\dot{\theta}_1,\dot{\theta}_2\in\mathcal{L}_\infty$. Thus, one can conclude that $\alpha_y=0$. In an analogous method, one has $\alpha_z=0$, and the following results are derived as

$$\alpha_y=0,\alpha_z=0\Rightarrow e_y=0,e_z=0. \tag{30}$$

Further, inserting (30) and (12) into (1), (2) and (4), one has

$$(m_h+m_c)\,l\left(\ddot{\theta}_1C_1-\dot{\theta}_1^2S_1\right)+m_cc\left(\ddot{\theta}_2C_2-\dot{\theta}_2^2S_2\right)=0, \tag{31}$$

$$(m_h+m_c)\,l\left(\ddot{\theta}_1S_1+\dot{\theta}_1^2C_1\right)+m_cc\left(\ddot{\theta}_2S_2+\dot{\theta}_2^2C_2\right)=0, \tag{32}$$

$$(m_h+m_c)\,l\left(l\ddot{\theta}_1+gS_1\right)+m_clc\left(\dot{\theta}_2^2S_{1-2}+\ddot{\theta}_2C_{1-2}\right)=0. \tag{33}$$

Subsequently, calculating (31) $\times C_1+$ (32) $\times S_1$ yields

$$(m_h+m_c)\,l\ddot{\theta}_1+m_cc\left(\dot{\theta}_2^2S_{1-2}+\ddot{\theta}_2C_{1-2}\right)=0. \tag{34}$$

Then, combining (34) with (33) and according to *Assumption 1*, one can obtain

$$(m_h+m_c)\,gS_1=0\Rightarrow\theta_1=0,\dot{\theta}_1=0,\ddot{\theta}_1=0. \tag{35}$$

Substituting (35) into (31) and (32) yields

$$m_cc\left(\ddot{\theta}_2C_2-\dot{\theta}_2^2S_2\right)=0, \tag{36}$$

$$m_cc\left(\ddot{\theta}_2S_2+\dot{\theta}_2^2C_2\right)=0, \tag{37}$$

from which one can further obtain that

$$(37)\times C_2-(36)\times S_2=0\Rightarrow\dot{\theta}_2=0\Rightarrow\ddot{\theta}_2=0. \tag{38}$$

Substituting (38), (35) and (23) into (5), and noting *Assumption 1*, one has

$$m_ccgS_2=0\Rightarrow\theta_2=0. \tag{39}$$

Finally, substituting (23), (35), (38) and (39) into (26) yields

$$-\alpha_l\left(k_{pl}+k_{sl}\beta_l\right)=0\Rightarrow\alpha_l=0\Rightarrow e_l=0. \tag{40}$$

Summarizing the results in (23), (35), (38), (39) and (40), the largest invariant set Λ contains merely the closed-loop equilibria. Thus, *Theorem 1* holds. ■

IV. SIMULATION RESULTS

In this section, simulation tests are implemented to verify the feasibility of the proposed control scheme. According to the constructed control input $\boldsymbol{u}$, the actual thrust input and the desired roll angle of the quadrotor is given as follows:

$$f=\sqrt{f_y^2+f_z^2},\ \phi_d=\arctan(-\frac{f_y}{f_z}).$$

The physical parameters of the ATSVC are set as $M=2.0\mathrm{kg}, m_h=0.2\mathrm{kg}, m_c=0.4\mathrm{kg}, c=0.3\mathrm{m}, g=9.8\mathrm{m/s}^2$. The controller without overshoot constraint is selected as the comparison method, with the specific form as follows:

$$\begin{aligned}\boldsymbol{u}_c=&-K_p\mathrm{Arctan}(\boldsymbol{e}_\eta)-K_d\mathrm{Arctan}(\boldsymbol{\epsilon}_\eta)\\&+(M+m_h+m_c)\,g\boldsymbol{r}_2-(m_h+m_c)\,g\boldsymbol{r}_3.\end{aligned}$$

The values of K_p and K_d for both the proposed method and the comparison method are selected to be the same. Specifically, the control gains are list as

$$k_{py}=1.2,k_{pz}=1.2,k_{pl}=1.0, \tag{41}$$

$$k_{dy}=2.5,k_{dz}=2.5,k_{dl}=1.6, \tag{42}$$

$$k_{sy}=0.2,k_{sz}=0.2,k_{sl}=0.1. \tag{43}$$

Two sets of numerical simulation tests are conducted by providing different initial and desired positions of the quadrotor, as well as lengths of the cable, i.e.,

1) *Simulation 1:* The initial quadrotor position and cable length are $y_0=5\mathrm{m}, z_0=3\mathrm{m}, l_0=8.5\mathrm{m}$, the desired quadrotor position and cable length are $y_d=2\mathrm{m}, z_d=7\mathrm{m}, l_d=3.5\mathrm{m}$. The allowable overshoot magnitudes are $\delta_y=0.4\mathrm{m}, \delta_z=0.25\mathrm{m}, \delta_l=0.45\mathrm{m}$. The results are presented in Fig. 2.
2) *Simulation 2:* The initial quadrotor position and cable length are $y_0=2\mathrm{m}, z_0=5\mathrm{m}, l_0=3\mathrm{m}$, the desired quadrotor position and cable length are $y_d=6\mathrm{m}, z_d=2.5\mathrm{m}, l_d=5\mathrm{m}$. The allowable overshoot magnitudes are $\delta_y=0.4\mathrm{m}, \delta_z=0.25\mathrm{m}, \delta_l=0.25\mathrm{m}$. The results are presented in Fig. 3.

From the simulation curves, one finds that both control schemes can realize quadrotor positioning, cable length adjusting and hook/cargo swing elimination. However, due to the overshoot constraint term imposed by the proposed

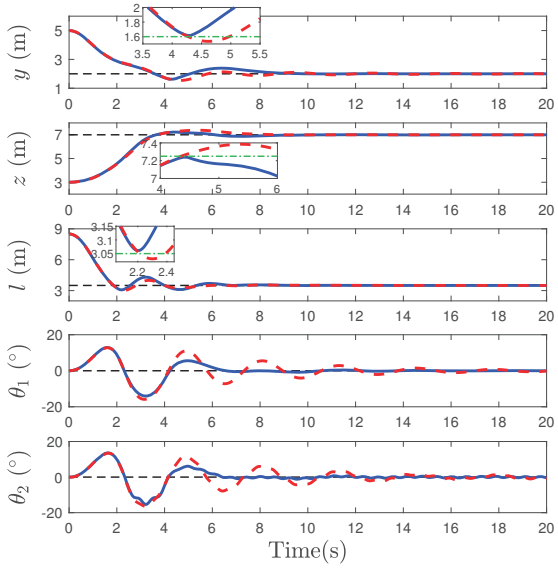

(a) Quadrotor position, hook and cargo swing angles.

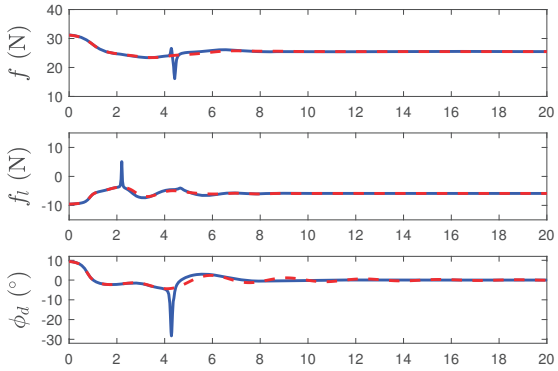

(b) Control inputs.

Fig. 2: Results for *Simulation 1*. (Black dotted lines: Desired states. Blue solid lines: Results by the proposed method. Red dotted lines: Results by the comparison method. Green dash dot lines: Allowable overshoot magnitude.)

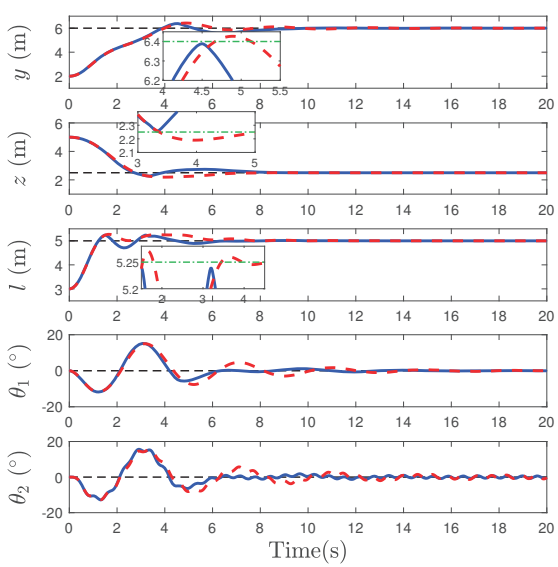

(a) Quadrotor position, hook and cargo swing angles.

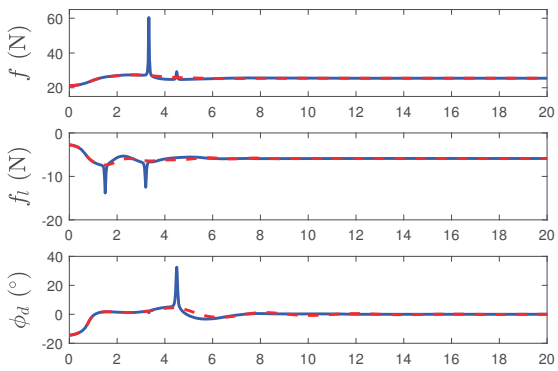

(b) Control inputs.

Fig. 3: Results for *Simulation 2*. (Black dotted lines: Desired states. Blue solid lines: Results by the proposed method. Red dotted lines: Results by the comparison method. Green dash dot lines: Allowable overshoot magnitude.)

method, the maximum overshoot of the quadrotor position and cable length is smaller than the comparison method. Furthermore, from the simulation results one can observe that the restrictions on overshoot also indirectly reduce the swing angles of the hook and cargo.

V. CONCLUSIONS

This paper investigates the output feedback control of double-pendulum ATSVC. Unlike conventional approaches, this method operates independently of velocity information and confines the quadrotor's overshoot within a prescribed scope. The stability of the closed-loop system is guaranteed by Lyapunov techniques and LaSalle's Invariance Theorem. Simulation results show the excellent performance in quadrotor positioning, cable length adjusting and hook/cargo swing elimination. In ensuring work, we will further establish the dynamic model in three-dimensional space and conduct cargo transportation tests in practical environments.

REFERENCES

[1] S. Yang, B. Xian, J. Cai, and G. Wang, "Finite-time convergence control for a quadrotor unmanned aerial vehicle with a slung load," *IEEE Transactions on Industrial Informatics*, vol. 20, no. 1, pp. 605–614, 2024.

[2] A. Akhtar, S. Saleem, and J. Shan, "Path following of a quadrotor with a cable-suspended payload," *IEEE Transactions on Industrial Electronics*, vol. 70, no. 2, pp. 1646–1654, 2023.

[3] D. Guo and K. K. Leang, "Image-based estimation, planning, and control of a cable-suspended payload for package delivery," *IEEE Robotics and Automation Letters*, vol. 5, no. 2, pp. 2698–2705, 2020.

[4] H. Yu, S. Wu, W. He, X. Liang, J. Han, and Y. Fang, "Fault-tolerant control for multirotor aerial transportation systems with blade damage," *IEEE Transactions on Industrial Electronics*, DOI 10.1109/TIE.2023.3347848, 2024.

[5] J. Zeng, P. Kotaru, and K. Sreenath, "Geometric control and differential flatness of a quadrotor uav with load suspended from a pulley," in *Proceedings of the 2019 American Control Conference (ACC)*, pp. 2420–2427. IEEE, 2019.
[6] X. Liang, H. Yu, Z. Zhang, H. Liu, Y. Fang, and J. Han, "Unmanned aerial transportation system with flexible connection between the quadrotor and the payload: modeling, controller design, and experimental validation," *IEEE Transactions on Industrial Electronics*, vol. 70, no. 2, pp. 1870–1882, 2023.
[7] J. Huang, H. Tao, Y. Wang, and J.-Q. Sun, "Suppressing uav payload swing with time-varying cable length through nonlinear coupling," *Mechanical Systems and Signal Processing*, vol. 185, p. 109790, 2023.
[8] K. Cai, H. Yu, W. He, X. Liang, J. Han, and Y. Fang, "An enhanced-coupling control method for aerial transportation systems with double-pendulum swing effects," *IEEE/ASME Transactions on Mechatronics*, DOI 10.1109/TMECH.2023.3316423, 2023.
[9] J. Qi, Y. Ping, M. Wang, and C. Wu, "Online trajectory planning method for double-pendulum quadrotor transportation systems," *Electronics*, vol. 11, no. 1, p. 50, 2021.
[10] K. K. Dhiman, Abhishek, and M. Kotharic, "Flight dynamics and control of an unmanned helicopter with underslung double pendulum," *Journal of Aircraft*, vol. 59, no. 1, pp. 137–153, 2022.
[11] J. Xia and H. Ouyang, "Amplitude saturated nonlinear output feedback controller design for underactuated 5-dof tower cranes without velocity measurement," *IEEE Transactions on Intelligent Transportation Systems*, DOI 10.1109/TITS.2024.3350056, 2024.
[12] H. K. Khalil, *Nonlinear systems*. Upper Saddle River, NJ, USA: Prentice-Hall, 2002.